

STATUS OF THE SPALLATION NEUTRON SOURCE ACCELERATOR COMPLEX*

Stuart Henderson

Spallation Neutron Source Project, Oak Ridge National Laboratory, USA

Abstract

The Spallation Neutron Source accelerator system will provide a 1-GeV, 1.44-MW proton beam to a liquid mercury target for neutron production. The accelerator complex consists of an H⁻ injector capable of producing a 38-mA peak current, a 1-GeV linear accelerator, an accumulator ring and associated transport lines. The linear accelerator consists of a drift-tube linac, a coupled-cavity linac and a superconducting linac which provide a 1.5-mA average current to the accumulator ring. The design of the accelerator systems is complete; installation of the accelerator components is in progress; and staged beam commissioning is proceeding as installation progresses. The installation and final commissioning of the project is on schedule for completion in early 2006. The status of the project design, installation and commissioning will be presented.

* SNS is managed by UT-Battelle, LLC, under contract DE-AC05-00OR22725 for the US Department of Energy. SNS is a partnership of six national laboratories: Argonne, Brookhaven, Jefferson, Lawrence Berkeley, Los Alamos and Oak Ridge.

Introduction

The Spallation Neutron Source (SNS) is a short-pulse neutron scattering facility under construction at Oak Ridge National Laboratory by the US Department of Energy. At 1.44 MW of proton beam power on target, the SNS will operate at powers a factor of 7 beyond that achieved at what is now the most intense short-pulse neutron source, the ISIS facility at Rutherford Appleton Laboratory in the UK [1]. The SNS is a partnership of six US DOE national laboratories, each of which is designing and manufacturing a portion of the facility. The project is now in a construction phase, with transition to operations expected in 2006.

The SNS accelerator complex [2] is composed of a 2.5-MeV H^- injector [3], a 1-GeV linear accelerator [4], an accumulator ring and associated beam transport lines [5]. The SNS baseline parameters are summarised in Table 1. The injector (also called the front-end systems) consists of an H^- volume ion-source with a 50-mA peak current capability, a radio-frequency quadrupole and a medium-energy beam transport line for chopping and matching the 2.5-MeV beam to the linac. The linear accelerator consists of a drift-tube linac (DTL) with an output energy of 87 MeV, a coupled-cavity linac (CCL) with an output energy of 187 MeV, and a superconducting RF linac (SCL) with 1-GeV output energy. The linac produces a 1-msec long, 38-mA peak, chopped beam pulse at 60 Hz for accumulation in the ring. The linac beam is transported via the high-energy beam transport (HEBT) line to the injection point in the accumulator ring, where the 1-msec long pulse is compressed to less than 1 microsecond by charge-exchange multi-turn injection. In baseline operation, beam is accumulated in the ring over 1 060 turns reaching an intensity of $1.5 \cdot 10^{14}$ protons per pulse. When accumulation is complete the extraction kicker fires during the 250-nsec gap to remove the accumulated beam in a single turn and direct it into the ring-to-target beam transport (RTBT) line, which takes the beam to a liquid-mercury target.

Table 1. SNS baseline parameters

Beam power on target	1.44 MW
Beam energy	1 000 MeV
Linac beam macropulse duty factor	6.0%
Beam pulse length	1.0 msec
Repetition rate	60 Hz
Chopper beam-on duty factor	68%
Peak macropulse H^- current	38 mA
Average linac H^- current	1.6 mA
Ring accumulation time	1 060 turns
Ring bunch intensity	$1.6 \cdot 10^{14}$
Ring space-charge tune spread	0.15
Beam pulse length on target	695 nsec

Staged commissioning of the accelerator complex is proceeding as installation progresses. At this point, construction of all accelerator tunnels and enclosures is complete. The final project construction effort is focused on the target and the central laboratory and office buildings. To date, the front-end systems and half the drift-tube linac have been beam commissioned. Table 2 summarises the main commissioning results, comparing beam measurements with design goals.

Table 2. Beam commissioning performance to date

	Baseline design or goal	Achieved in commissioning
DTL1 peak current [mA]	38	40
DTL1-3 peak current [mA]	38	38
DTL1 beam pulse length [msec]	1.0	1.0
DTL1 average current [mA]	1.6	1.05
DTL1 horizontal emittance [p mm mrad (RMS, norm.)]	0.3	0.30 (fit), 0.40 (RMS)
DTL1 vertical emittance [p mm mrad (RMS, norm.)]	0.3	0.21 (fit), 0.31 (RMS)
DTL1 duty factor	6.0%	4.0%
MEBT beam energy [MeV]	2.5	2.45 – 0.010
DTL2 output energy [MeV]	22.89	22.94 – 0.11

Front-end status

The front-end systems were designed and built by Lawrence Berkeley National Laboratory (LBNL), commissioned at LBNL in May 2002, and reassembled and recommissioned at ORNL in late 2002. The front end consists of a volume H⁻ ion source with a 50-mA peak current, 6% duty factor and an electrostatic low-energy beam transport (LEBT) line to provide a properly matched, 65-keV beam for injection into the RFQ. Pre-chopping is performed by the LEBT chopper which deflects 32% of the beam onto the front face of the RFQ with a rise/fall time of 40 nsec. The RFQ is designed for a 38-mA peak output current, operates at 402.5 MHz and provides a 2.5-MeV output beam energy. The medium-energy beam is transported to the drift-tube linac via the MEBT, which contains four RF rebuncher cavities to properly match the beam longitudinally, a set of matching quadrupoles, and a fast chopper system with 10 nsec rise/fall time to remove the “partially chopped” beam from the LEBT chopper and further reduce the beam extinction ratio to below 10⁻⁴.

A peak MEBT output current of 50 mA was demonstrated, surpassing the design goal of 38 mA. In subsequent DTL commissioning, the front-end systems have operated at full 1 msec pulse length, and provided a 1-mA average current (4% duty factor) beam for injection into the DTL. The MEBT output beam emittances were measured and found to be in the range of 0.25-0.30 p mm-mrad (RMS, normalised) which meets the specification. Additionally, the MEBT output energy was measured and found to be 2.45 – 0.01 MeV, compared with the 2.5-MeV nominal, design energy.

The MEBT contains a number of beam diagnostic devices which are, or will be, important for characterising the beam parameters prior to injection into the linac. In addition to beam position monitors and wire scanners, a diagnostics box is being commissioned with an in-line slit/harp emittance measurement station, a 3-D beam profile system based on a mode-locked laser, and a fast-faraday cup for measurement of the longitudinal beam profile.

Linac status

The linac consists of three sections: the DTL, the CCL and the SCL. The DTL, CCL as well as all the high-power RF systems for the linac were designed and procured by Los Alamos National Laboratory (LANL).

DTL status and commissioning results

The drift-tube linac consists of six accelerating tanks with a final output energy of 87 MeV. The DTL operates at 402.5 MHz, the same bunch frequency as the RFQ. Tanks are individually powered with klystrons of 2.5-MW peak power and 8% duty factor capability. The transverse focusing is arranged in a FFODDO lattice utilising permanent-magnet quadrupoles. Some empty drift tubes contain beam position monitors and dipole correctors. The inter-tank sections contain toroidal beam current monitors, wire scanners and energy degrader/faraday cups.

To date, the entire DTL has been RF-tuned and installed in the linac tunnel. DTL tank tuning has resulted in longitudinal fields within the specification of -1% of design. The first three DTL tanks have been commissioned with beam.

The first three of six DTL tanks have been commissioned with beam in two separate runs. In the first run, DTL tank 1 (output energy 7.5 MeV) was commissioned into a dedicated diagnostics system (the “D-plate”) equipped with a full-power beam stop. In the second commissioning run, DTL tanks 1-3 (output energy 40 MeV) were commissioned into a low-power beam stop. The goals of the commissioning runs have been to demonstrate full system functionality, demonstrate beam acceleration with design beam parameters to the limits of the available beam stop, test and validate beam commissioning algorithms, and commission the installed diagnostic devices.

The basic procedure for setting the RF phase and amplitude of the DTL tanks relies on installed energy degrader/faraday cups (ED/FC) after each tank. A thin carbon absorber with thickness chosen to absorb low-energy beam particles is placed in front of a faraday cup (FC), and the FC signal is recorded as a function of the tank phase and amplitude. The phase is obtained by maximising the transmitted (on-energy) beam current, while the amplitude is determined by comparing the measured phase-width of the transmitted current with simulation predictions.

For the DTL1 beam commissioning run, a dedicated diagnostics system with energy degrader/faraday cups, wire scanners, beam position monitors, slit/harp emittance system and a bunch-shape monitor was installed following the tank to enable detailed characterisation of the output beam parameters. Following this short diagnostics beam line was a full beam-power beam stop.

Table 2 summarises the DTL commissioning results. The design peak current of 38 mA was readily achieved. A 1-msec long beam pulse was generated at a 20-mA average current during the pulse (at low duty factor). Finally, a 1-mA average current beam was accelerated in DTL1 with 100% beam transmission. For this demonstration, a beam pulse of 26-mA peak current, 650-microsecond pulse length at 60 Hz (7.5-kW beam power) was achieved. Figure 1 shows an overlay of beam current monitor signals in the MEBT and DTL1 during this high-power operation.

Extensive DTL1 output beam emittance measurements were performed. Figure 2 shows a vertical emittance measurement at a 38-mA peak current. The data are analysed in two ways. First, a Gaussian fit is performed to the two-dimensional beam distribution in position-angle space to obtain an emittance that is representative of the beam core. Values obtained in this way are 0.21 p mm mrad (RMS, normalised) in the vertical plane and 0.30 p mm mrad in the horizontal plane. In a second analysis, the RMS of the beam distribution is calculated with a 1% threshold (relative to the peak beam intensity) to remove spurious noise. Values obtained in this way are somewhat larger than the core emittances: 0.31 p mm mrad, and 0.40 p mm mrad in the vertical and horizontal, respectively. Further analysis of the large set of emittance data is in process.

DTL tanks 1-3, with output energies of 40 MeV, were recently beam commissioned. Again, peak currents of 38 mA transported through all three tanks with 100% transmission were demonstrated. The beam stop limited beam pulse lengths to less than 50 microseconds, and repetition rates to 1 Hz.

Figure 1. Overlay of beam current monitors after the RFQ, MEBT, DTL1 and at the beam stop, respectively. The data were recorded during the 1-mA average current, high-power run.

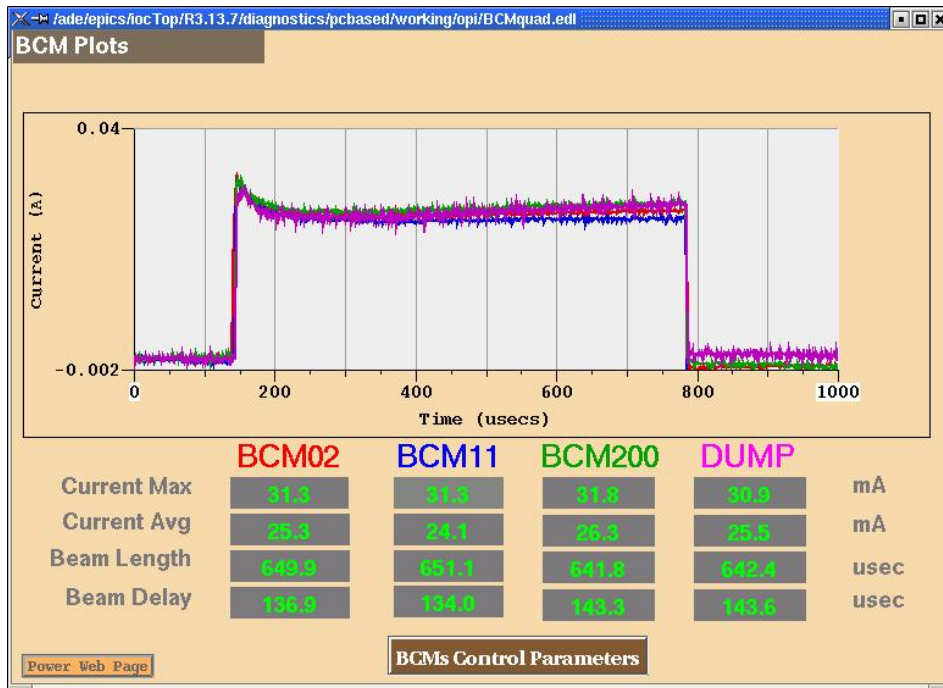
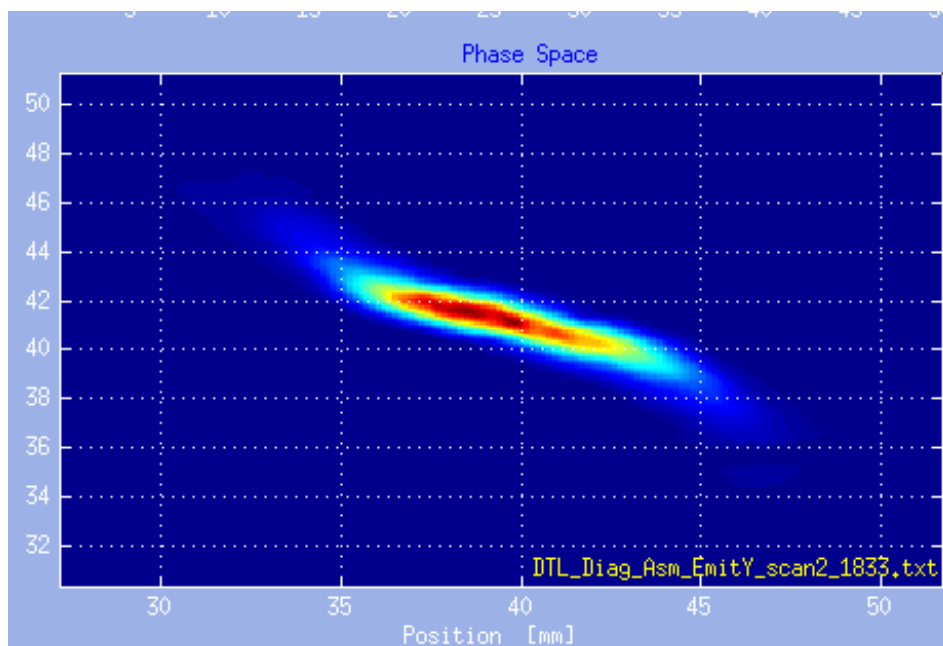


Figure 2. DTL tank 1 vertical output emittance at 38-mA peak current. Angle (mrad) is plotting vs. position (mm).



Coupled-cavity linac status

The CCL consists of four modules, each containing 12 segments (coupled by bridge couplers) driven in the $\pi/2$ mode. The CCL operates at 805 MHz, double the frequency of the upstream linac components. Each module is powered in two locations with a single 5-MW peak power klystron. The inter-segment spaces contain quadrupoles, dipole correctors and a suite of diagnostic devices, including beam position monitors, wire scanners, and bunch-shape monitors for measuring the longitudinal beam profile.

The coupled-cavity linac modules have been manufactured, delivered and installed in the tunnel. The first two modules have been RF-tuned, and the last two modules are being tuned. CCL module 1 was RF-processed up to the design accelerating field in approximately two days. Installation of the remaining CCL beam line hardware is in progress. The complete DTL and CCL linacs will be commissioned in August 2004.

Superconducting linac status

The superconducting linac is being built by the Thomas Jefferson National Accelerator Facility. The SCL utilises six-cell elliptical π -mode superconducting niobium accelerating cavities. Two structures, one with matched velocity $\beta = 0.61$ (the medium-beta cavity), and another with matched $\beta = 0.81$ (the high-beta cavity) are used in the SCL. The medium-beta portion of the SCL consists of 33 cavities in 11 cryomodules, and the high-beta portion consists of 48 cavities in 12 cryomodules. The peak surface field in the medium-beta cavities is 27 MV/m, giving an accelerating gradient of 10.2 MV/m for the matched particle. In the high-beta cavities, the nominal peak surface fields are 35 MV/m, giving 15.6 MV/m accelerating gradient. The quality factor is greater than $5 \cdot 10^9$. The transverse focusing is accomplished with a doublet focusing lattice located in the warm sections between cryomodules. Each RF cavity in the SCL is independently powered by a single 550-kW klystron. This powering scheme maximises the flexibility of the SCL, providing the ability to drive well-performing cavities harder, and “tune-around” cavities that may be unpowered. In addition to beam position monitors, a laser-based beam profile system is being utilised [6].

To date, all medium-beta cryomodules have been constructed, and eight have been installed in the tunnel on the SNS site. All cavities have exceeded the specified accelerating gradient and quality factor. The high-beta cryomodules are in full production. Recently, 4.5 K liquid He was made in the central helium liquifier (CHL). CHL commissioning is underway and it is expected that the first cryomodule will be cooled down in late summer 2004. Testing of cryomodules in the linac tunnel will proceed through late 2004, with beam commissioning of the SCL scheduled for March 2005.

Ring and transport lines status

The ring and transport line systems were designed by Brookhaven National Laboratory (BNL). The H^- beam from the linac is transported to the ring in the high-energy beam transport (HEBT) line. Before the 90° bend in the HEBT is a tuning beam dump (the linac dump) which will be used for linac commissioning and linac tune-up during operations. The HEBT delivers the beam to the stripping foil for charge-exchange injection into the accumulator ring. Un-stripped H^- and partially stripped (H^0) beams are fully stripped in a second foil and transported to the injection dump via the injection dump line. The injection dump is designed to handle 10% of the design beam power (150 kW) that can be expected from the combination of stripping inefficiency and linac beam that misses the foil. Also included in the HEBT are transverse and longitudinal collimation systems which remove the beam halo and deposit those particles in fixed absorbers.

The ring is a four-fold symmetric lattice with long straight sections each with a dedicated function. The injection systems are contained in one straight section, fixed collimators are located in another, the extraction systems populate the third, and the RF systems are contained in the fourth section. The 1-msec long beam pulse from the linac is accumulated over 1 060 turns in the ring by charge-exchange multi-turn injection. Phase-space painting is utilised in all three dimensions. In the transverse, sets of horizontal and vertical injection kickers are used to ramp the closed orbit away from the injection foil during accumulation. Longitudinal painting is accomplished with an energy spreader cavity. The beam is captured in a single $h = 1$ RF bucket of 40-kV amplitude with a dual-harmonic ($h = 2$) amplitude of 20 kV to increase the bunch factor.

Central to achieving low loss in the ring is adequate vacuum chamber aperture and an efficient collimation system [7]. The uncontrolled beam loss criteria for the ring is 1 W/m, which amounts to about 10^{-4} fractional uncontrolled beam loss. The vacuum chamber aperture is everywhere at least 480 μ mm mrad, with the exception of the fixed collimators, which provide limiting horizontal and vertical apertures of 300 μ mm mrad in heavily shielded and water-cooled collimator assemblies. Phase-space painting is performed in all three dimensions to a resulting transverse emittance of about 200 μ mm mrad. The collimation system is “two-stage” in the sense that beam halo particles first strike a fixed scraper, placed at about 240 μ mm mrad, propelling these particles to large amplitude, so that they are removed at the fixed collimators. Simulations show that about 10^{-3} of the beam particles strike the primary scraper, and about 90% of those are absorbed in the fixed collimators, with the other 10% giving rise to uncontrolled beam loss at a level of 10^{-4} of the beam.

Once accumulation is complete, a set of single-turn kickers are fired to deflect the accumulated beam into the ring-to-target beam (RTBT) transport line which takes the beam to the liquid mercury target. Located midway along the RTBT is another tuning beam dump (the extraction dump) with a 7.5-kW beam power capability.

The HEBT beam line is almost completely installed and the straight portion is under vacuum. The ring arcs are delivered in “half-cell” assemblies which contain one dipole, one quadrupole and associated correctors and their beam pipes. Twenty-five (25) of the 32 half-cells have been delivered and installed in the tunnel. Ring power supply production is in full swing and power supply delivery has commenced. Ring high-power RF systems have been built and the first has been delivered to ORNL. The injection magnet systems are built and an assembly test is underway. The collimation systems are being delivered to ORNL. Ring beam commissioning up to the extraction beam dump is scheduled for June-November 2005. Commissioning of the final portion of the RTBT and the liquid mercury target itself is scheduled for February 2006 in order to declare project construction completion in March 2006.

REFERENCES

- [1] Prior, C., *et al.*, *Proc. Part. Acc. Conf. 2003*, p. 1527.
- [2] Holtkamp, N., *Proc. Part. Acc. Conf. 2003*, p. 11.
- [3] Aleksandrov, A., *Proc. Part. Acc. Conf. 2003*, p. 65.
- [4] Jeon, D., *Proc. Part. Acc. Conf. 2003*, p. 107.
- [5] Wei, J., *Proc. Part. Acc. Conf. 2003*, p. 571.
- [6] Assadi, S., *Proc. Part. Acc. Conf. 2003*, p. 2706.
- [7] Cousineau, S., *et. al.*, *Proc. Eur. Part. Acc. Conf. 2002*.

TECHNICAL SESSION II

Target, Window and Coolant Technology

Chairs: X. Cheng, T-Y. Song

TABLE OF CONTENTS

Foreword	3
Executive Summary.....	11
Welcome.....	15
<i>D-S. Yoon</i> Congratulatory Address	17
<i>I-S. Chang</i> Welcome Address	19
<i>G.H. Marcus</i> OECD Welcome	21
GENERAL SESSION: ACCELERATOR PROGRAMMES AND APPLICATIONS.....	23
<i>CHAIRS: B-H. CHOI, R. SHEFFIELD</i>	
<i>T. Mukaiyama</i> Background/Perspective.....	25
<i>M. Salvatores</i> Accelerator-driven Systems in Advanced Fuel Cycles	27
<i>S. Noguchi</i> Present Status of the J-PARC Accelerator Complex	37
<i>H. Takano</i> R&D of ADS in Japan.....	45
<i>R.W. Garnett, A.J. Jason</i> Los Alamos Perspective on High-intensity Accelerators.....	57
<i>J-M. Lagniel</i> French Accelerator Research for ADS Developments.....	69
<i>T-Y. Song, J-E. Cha, C-H. Cho, C-H. Cho, Y. Kim, B-O. Lee, B-S. Lee, W-S. Park, M-J. Shin</i> Hybrid Power Extraction Reactor (HYPER) Project	81

<i>V.P. Bhatnagar, S. Casalta, M. Hugon</i> Research and Development on Accelerator-driven Systems in the EURATOM 5 th and 6 th Framework Programmes.....	89
<i>S. Monti, L. Picardi, C. Rubbia, M. Salvatores, F. Troiani</i> Status of the TRADE Experiment.....	101
<i>P. D'hondt, B. Carlucci</i> The European Project PDS-XADS “Preliminary Design Studies of an Experimental Accelerator-driven System”.....	113
<i>F. Groeschel, A. Cadiou, C. Fazio, T. Kirchner, G. Laffont, K. Thomsen</i> Status of the MEGAPIE Project.....	125
<i>P. Pierini, L. Burgazzi</i> ADS Accelerator Reliability Activities in Europe	137
<i>W. Gudowski</i> ADS Neutronics	149
<i>P. Coddington</i> ADS Safety	151
<i>Y. Cho</i> Technological Aspects and Challenges for High-power Proton Accelerator-driven System Application.....	153
TECHNICAL SESSION I: ACCELERATOR RELIABILITY.....	163
<i>CHAIRS: A. MUELLER, P. PIERINI</i>	
<i>D. Vandeplasseche, Y. Jongen (for the PDS-XADS Working Package 3 Collaboration)</i> The PDS-XADS Reference Accelerator	165
<i>N. Ouchi, N. Akaoka, H. Asano, E. Chishiro, Y. Namekawa, H. Suzuki, T. Ueno, S. Noguchi, E. Kako, N. Ohuchi, K. Saito, T. Shishido, K. Tsuchiya, K. Ohkubo, M. Matsuoka, K. Sennyu, T. Murai, T. Ohtani, C. Tsukishima</i> Development of a Superconducting Proton Linac for ADS.....	175
<i>C. Miélot</i> Spoke Cavities: An Asset for the High Reliability of a Superconducting Accelerator; Studies and Test Results of a $\beta = 0.35$, Two-gap Prototype and its Power Coupler at IPN Orsay	185
<i>X.L. Guan, S.N. Fu, B.C. Cui, H.F. Ouyang, Z.H. Zhang, W.W. Xu, T.G. Xu</i> Chinese Status of HPPA Development	195

<i>J.L. Biarrotte, M. Novati, P. Pierini, H. Safa, D. Uriot</i> Beam Dynamics Studies for the Fault Tolerance Assessment of the PDS-XADS Linac	203
<i>P.A. Schmelzbach</i> High-energy Beat Transport Lines and Delivery System for Intense Proton Beams	215
<i>M. Tanigaki, K. Mishima, S. Shiroya, Y. Ishi, S. Fukumoto, S. Machida, Y. Mori, M. Inoue</i> Construction of a FFAG Complex for ADS Research in KURRI	217
<i>G. Ciavola, L. Celona, S. Gammino, L. Andò, M. Presti, A. Galatà, F. Chines, S. Passarello, XZh. Zhang, M. Winkler, R. Gobin, R. Ferdinand, J. Sherman</i> Improvement of Reliability of the TRASCO Intense Proton Source (TRIPS) at INFN-LNS	223
<i>R.W. Garnett, F.L. Krawczyk, G.H. Neuschaefer</i> An Improved Superconducting ADS Driver Linac Design.....	235
<i>A.P. Durkin, I.V. Shumakov, S.V. Vinogradov</i> Methods and Codes for Estimation of Tolerance in Reliable Radiation-free High-power Linac	245
<i>S. Henderson</i> Status of the Spallation Neutron Source Accelerator Complex	257
TECHNICAL SESSION II: TARGET, WINDOW AND COOLANT TECHNOLOGY.....	265
CHAIRS: X. CHENG, T-Y. SONG	
<i>Y. Kurata, K. Kikuchi, S. Saito, K. Kamata, T. Kitano, H. Oigawa</i> Research and Development on Lead-bismuth Technology for Accelerator-driven Transmutation System at JAERI	267
<i>P. Michelato, E. Bari, E. Cavaliere, L. Monaco, D. Sertore, A. Bonucci, R. Giannantonio, L. Cinotti, P. Turroni</i> Vacuum Gas Dynamics Investigation and Experimental Results on the TRASCO ADS Windowless Interface	279
<i>J-E. Cha, C-H. Cho, T-Y. Song</i> Corrosion Tests in the Static Condition and Installation of Corrosion Loop at KAERI for Lead-bismuth Eutectic	291
<i>P. Schuurmans, P. Kupschus, A. Verstrepen, J. Cools, H. Ait Abderrahim</i> The Vacuum Interface Compatibility Experiment (VICE) Supporting the MYRRHA Windowless Target Design	301

<i>C-H. Cho, Y. Kim, T-Y. Song</i> Introduction of a Dual Injection Tube for the Design of a 20 MW Lead-bismuth Target System.....	313
<i>H. Oigawa, K. Tsujimoto, K. Kikuchi, Y. Kurata, T. Sasa, M. Umeno, K. Nishihara, S. Saito, M. Mizumoto, H. Takano, K. Nakai, A. Iwata</i> Design Study Around Beam Window of ADS.....	325
<i>S. Fan, W. Luo, F. Yan, H. Zhang, Z. Zhao</i> Primary Isotopic Yields for MSDM Calculations of Spallation Reactions on ²⁸⁰ Pb with Proton Energy of 1 GeV.....	335
<i>N. Tak, H-J. Neitzel, X. Cheng</i> CFD Analysis on the Active Part of Window Target Unit for LBE-cooled XADS.....	343
<i>T. Sawada, M. Orito, H. Kobayashi, T. Sasa, V. Artisyuk</i> Optimisation of a Code to Improve Spallation Yield Predictions in an ADS Target System.....	355
TECHNICAL SESSION III: SUBCRITICAL SYSTEM DESIGN AND ADS SIMULATIONS.....	363
<i>CHAIRS: W. GUDOWSKI, H. OIGAWA</i>	
<i>T. Misawa, H. Unesaki, C.H. Pyeon, C. Ichihara, S. Shiroya</i> Research on the Accelerator-driven Subcritical Reactor at the Kyoto University Critical Assembly (KUCA) with an FFAG Proton Accelerator.....	365
<i>K. Nishihara, K. Tsujimoto, H. Oigawa</i> Improvement of Burn-up Swing for an Accelerator-driven System	373
<i>S. Monti, L. Picardi, C. Ronsivalle, C. Rubbia, F. Troiani</i> Status of the Conceptual Design of an Accelerator and Beam Transport Line for Trade.....	383
<i>A.M. Degtyarev, A.K. Kalugin, L.I. Ponomarev</i> Estimation of some Characteristics of the Cascade Subcritical Molten Salt Reactor (CSMSR).....	393
<i>F. Roelofs, E. Komen, K. Van Tichelen, P. Kupschus, H. Ait Abderrahim</i> CFD Analysis of the Heavy Liquid Metal Flow Field in the MYRRHA Pool.....	401
<i>A. D'Angelo, B. Arien, V. Sobolev, G. Van den Eynde, H. Ait Abderrahim, F. Gabrielli</i> Results of the Second Phase of Calculations Relevant to the WPPT Benchmark on Beam Interruptions	411

TECHNICAL SESSION IV: SAFETY AND CONTROL OF ADS 423

CHAIRS: J-M. LAGNIEL, P. CODDINGTON

*P. Coddington, K. Mikityuk, M. Schikorr, W. Maschek,
R. Sehgal, J. Champigny, L. Mansani, P. Meloni, H. Wider*
Safety Analysis of the EU PDS-XADS Designs..... 425

*X-N. Chen, T. Suzuki, A. Rineiski, C. Matzerath-Boccaccini,
E. Wiegner, W. Maschek*
Comparative Transient Analyses of Accelerator-driven Systems
with Mixed Oxide and Advanced Fertile-free Fuels 439

P. Coddington, K. Mikityuk, R. Chawla
Comparative Transient Analysis of Pb/Bi
and Gas-cooled XADS Concepts 453

B.R. Sehgal, W.M. Ma, A. Karbojian
Thermal-hydraulic Experiments on the TALL LBE Test Facility 465

K. Nishihara, H. Oigawa
Analysis of Lead-bismuth Eutectic Flowing into Beam Duct..... 477

P.M. Bokov, D. Ridikas, I.S. Slessarev
On the Supplementary Feedback Effect Specific
for Accelerator-coupled Systems (ACS)..... 485

W. Haeck, H. Ait Abderrahim, C. Wagemans
 K_{eff} and K_s Burn-up Swing Compensation in MYRRHA 495

TECHNICAL SESSION V: ADS EXPERIMENTS AND TEST FACILITIES 505

CHAIRS: P. D'HONDT, V. BHATNAGAR

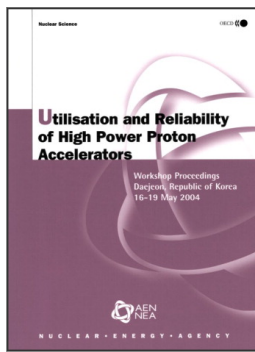
*H. Oigawa, T. Sasa, K. Kikuchi, K. Nishihara, Y. Kurata, M. Umeno,
K. Tsujimoto, S. Saito, M. Futakawa, M. Mizumoto, H. Takano*
Concept of Transmutation Experimental Facility 507

M. Hron, M. Mikisek, I. Peka, P. Hosnedl
Experimental Verification of Selected Transmutation Technology and Materials
for Basic Components of a Demonstration Transmuter with Liquid Fuel
Based on Molten Fluorides (Development of New Technologies for
Nuclear Incineration of PWR Spent Fuel in the Czech Republic) 519

Y. Kim, T-Y. Song
Application of the HYPER System to the DUPIC Fuel Cycle..... 529

M. Plaschy, S. Pelloni, P. Coddington, R. Chawla, G. Rimpault, F. Mellier
Numerical Comparisons Between Neutronic Characteristics of MUSE4
Configurations and XADS-type Models 539

<i>B-S. Lee, Y. Kim, J-H. Lee, T-Y. Song</i> Thermal Stability of the U-Zr Fuel and its Interfacial Reaction with Lead	549
SUMMARIES OF TECHNICAL SESSIONS	557
<i>CHAIRS: R. SHEFFIELD, B-H. CHOI</i>	
<i>Chairs: A.C. Mueller, P. Pierini</i> Summary of Technical Session I: Accelerator Reliability	559
<i>Chairs: X. Cheng, T-Y. Song</i> Summary of Technical Session II: Target, Window and Coolant Technology	565
<i>Chairs: W. Gudowski, H. Oigawa</i> Summary of Technical Session III: Subcritical System Design and ADS Simulations.....	571
<i>Chairs: J-M. Lagniel, P. Coddington</i> Summary of Technical Session IV: Safety and Control of ADS	575
<i>Chairs: P. D'hondt, V. Bhatagnar</i> Summary of Technical Session V: ADS Experiments and Test Facilities.....	577
SUMMARIES OF WORKING GROUP DISCUSSION SESSIONS	581
<i>CHAIRS: R. SHEFFIELD, B-H. CHOI</i>	
<i>Chair: P.K. Sigg</i> Summary of Working Group Discussion on Accelerators.....	583
<i>Chair: W. Gudowski</i> Summary of Working Group Discussion on Subcritical Systems and Interface Engineering	587
<i>Chair: P. Coddington</i> Summary of Working Group Discussion on Safety and Control of ADS.....	591
<i>Annex 1: List of workshop organisers</i>	<i>595</i>
<i>Annex 2: List of participants.....</i>	<i>597</i>



From:

Utilisation and Reliability of High Power Proton Accelerators

Workshop Proceedings, Daejeon, Republic of Korea, 16-19 May 2004

Access the complete publication at:

<https://doi.org/10.1787/9789264013810-en>

Please cite this chapter as:

Henderson, Stuart (2006), "Status of the Spallation Neutron Source Accelerator Complex", in OECD/Nuclear Energy Agency, *Utilisation and Reliability of High Power Proton Accelerators: Workshop Proceedings, Daejeon, Republic of Korea, 16-19 May 2004*, OECD Publishing, Paris.

DOI: <https://doi.org/10.1787/9789264013810-28-en>

This work is published under the responsibility of the Secretary-General of the OECD. The opinions expressed and arguments employed herein do not necessarily reflect the official views of OECD member countries.

This document and any map included herein are without prejudice to the status of or sovereignty over any territory, to the delimitation of international frontiers and boundaries and to the name of any territory, city or area.

You can copy, download or print OECD content for your own use, and you can include excerpts from OECD publications, databases and multimedia products in your own documents, presentations, blogs, websites and teaching materials, provided that suitable acknowledgment of OECD as source and copyright owner is given. All requests for public or commercial use and translation rights should be submitted to rights@oecd.org. Requests for permission to photocopy portions of this material for public or commercial use shall be addressed directly to the Copyright Clearance Center (CCC) at info@copyright.com or the Centre français d'exploitation du droit de copie (CFC) at contact@cfcopies.com.